TWO-DIMENSIONAL SIMULATIONS OF MAGMA INTERACTION WITH SUBSURFACE TUNNELS

Debashis Basu,[1] Kaushik Das,[1] and Stephen Self[2]

[1]*Center for Nuclear Waste Regulatory Analyses*
Southwest Research Institute®
San Antonio, Texas 78238

[2]*U.S. Nuclear Regulatory Commission*
Washington, DC

Contact: D. Basu, dbasu@swri.org, Telephone: +1-210-522-8333

A two-dimensional model is presented for magma ascending in an igneous dike and subsequently flowing into a dry horizontal subsurface tunnel containing obstacles. Computational Fluid Dynamics (CFD) analyses were performed to numerically assess magma dynamics inside the horizontal tunnel assuming transient effusive flow of single-phase (liquid, gas-free) magma. The numerical models were not designed to simulate the magmatic conditions of initial intersection or investigate possible changes to the properties of the leading magma to arrive at the tunnel, but rather the conditions after intersection, in a simple case where the tunnel is effusively invaded and filled with low-viscosity, liquid-dominated basaltic (low silica content) magma. Simulation results show that magma ascending along a dike that intersects a tunnel will fill the tunnel under the influence of gravity from the base to the top and then continue upwards along the dike or conduit. Counterrotating vortices adjacent to the dike that extend into the tunnel are driven by viscous coupling between the magma rising in the dike and existing magma that filled the tunnel. The computed results show that the complexity of the volcanic plumbing influences the pattern of the circulation developed in the tunnel. The pattern of circulation is largely influenced by the interplay between the ascending magma and location of the obstacles.

I. INTRODUCTION

The flow of magma through a subvolcanic plumbing system to the ground surface takes place through a complex network of dikes and sills. These magma pathways connect the deeper regions of magma accumulation inside the Earth's crust with the surface. Magma flow through dikes and sills also depends on the depth (pressure) of the magma, on the internal properties of the magma (e.g., viscosity, developed and exsolved gas content), and on the geological as well as structural characteristics of the surrounding rock.[1] In the near subsurface, conduits develop at the tops of dikes (and sometimes sills) that connect the magma column to the surface volcanic vent. These are wider than the dike and usually flare upwards. Conduit shape reflects, and is controlled by, the rapidly changing properties of the magma (e.g., degassing and bubble growth, expansion, cooling, crystallization) as it nears the low-pressure surface interface. Low viscosity or basaltic magmas often erupt effusively from fissures and vents, whereas the more viscous silicic magmas erupt explosively, forming pyroclastic products from (usually) central vents that are also fed by dikes tapping magma reservoirs. In many cases with basaltic igneous activity, magma rise along a dike system is essentially a homogeneous flow until the gas concentration becomes sufficiently large and/or external perturbations cause magma fragmentation within the conduit.[2,3] The modeling case developed here is appropriate for conditions of basaltic magma flow beneath the depth at which a volcanic conduit would typically develop[4] and is thus intended to examine only the interaction of a magma-filled dike intersecting and crossing a tunnel.

The modeling of basaltic magma ascent dynamics through dikes is moderately well developed, documented, and understood.[5-8] Typical assumptions inherent in the simulations include the steady, one-dimensional, isothermal, single or multiphase nonequilibrium flows. Several researchers[9-11] have also predicted explosive volcanic flows involving nonlinear, transient, multidimensional, multiphase dynamics, including flow in tunnels[12], that evolve over a range of spatial and temporal scales. However, none of the previous simulations modeled the interaction of basaltic magma with a subsurface tunnel in the presence of an

obstacle to effusive magma flow. Previous work by several researchers[13-17] focusing on various aspects of interaction between a dike and a subsurface tunnel have collectively shown that a tunnel intersected by ascending basaltic magma will quickly fill with magma and concluded that physical conditions such as the velocity of the magma and the static and dynamic pressure inside the tunnel will be influenced by the magma.

Menand, et al.[13] simulated the flow of viscous bubbly liquid in a configuration analogous to a tunnel without obstacles intersected by a dike using an experimental study with analog fluid (golden syrup) that scales to low-viscosity basaltic magma. They showed that circulation would develop in the tunnel, with the primary vortex closest to the entrance of the cavity being the strongest and the strength of the successive vortices decreasing down the tunnel. They also showed that foam developed from degassing (bubble growth) could change the flow style in the tunnel. Another study[15], examines possibilities when degassed magma invades a tunnel and shows that slow flow could fill, or partially fill the void space. The present research goes beyond the work described above and examines circulation patterns that might develop in basaltic magma flowing inside a subsurface tunnel in the presence of obstacles. One previous study[18] that presents an alternative scenario is specific to the proposed Yucca Mountain geologic nuclear waste repository and proposes that relatively high-volatile-content basaltic magma would cool and crystallize rapidly when it enters a tunnel, thus blocking further flow of magma for any significant distance.

The present paper also analyzes the effect of magma velocity and obstacle position inside a tunnel on the predicted velocity field and circulation pattern. It presents results of computational analyses designed to investigate the flow of magma into a dry horizontal subsurface tunnel including obstacles after intersection with the tunnel during initial ascent of a dike. Applications of this work are to assessment of hazards should a subsurface tunnel in a region of active volcanism be invaded by a dike. Specific cases could be a mined nuclear waste repository with near-horizontal drifts or tunnels, or road and rail tunnels. In the case of a waste repository the obstacles would be waste packages or disposal containers designed to isolate radioactive waste over extended periods.

II. MODEL GEOMETRY AND CONFIGURATION

The configuration modeled in this study was restricted to two dimensions. As seen in Fig. 1, a 600-m (1,970-ft)-long by 6-m (20-ft) diameter horizontal circular tunnel is intersected at its midpoint by a vertical 8 m wide (26.25 ft) dike. In the model geometry, the dike extends more than 500 m (1,640.42 ft) below and 300 m (984 ft) above the subsurface tunnel. The dike width and length of the tunnel was based on information available in the

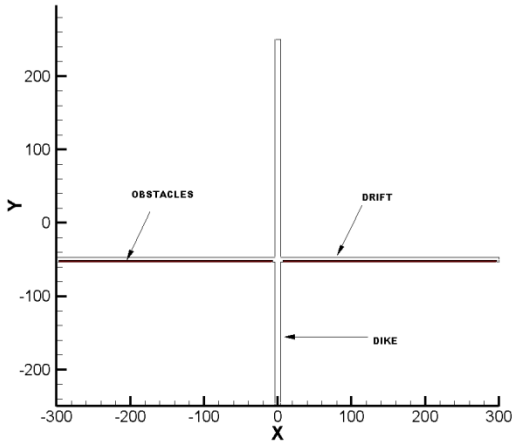

Fig. 1. Schematic of the model configuration

open literature.[19] In these simulations, to enhance numerical stability of the solution, two large, solid obstacles were used: one placed on either side of the intersected tunnel and each 290 m (951.443 ft) long and 1.8 m (5.9 ft) in height. The geometric dimensions of the tunnel and the obstacles were based on information available in the open literature.[19-21] and are provided in Table I. The dimensions of the dike and tunnel at the intersection are sufficient to model moderate magma supply rates (~ 10 to 50 m^3/s) for a basaltic eruption at a magma rise rate up to a few m/s, based on values observed at modern, active basaltic volcanoes.

III. COMPUTATIONAL GRID

The two-dimensional uniform computational grid used in these simulations consisted of 21,186 hexahedral cells (Fig. 2). Table II provides the details of the grid dimensions for each geometric construct. A velocity boundary condition was applied at the dike bottom inlet with velocities ranging between 1–3 m/s (3.3–9.8 ft/s), a pressure outlet boundary condition was applied at the dike top outlet with the pressure specified as atmospheric, and a no-slip boundary condition was applied at the walls. The volumetric flow rate that is possible with this velocity range is large for a basaltic intrusion/eruption (over such a small area), which is around 250-750 m^3/sec.

TABLE I. Model Construct Values

Construct	Value
Drift Length	600 m (1,970 ft)
Drift Height	6 m (20 ft)
Dike Length Below Drift	>500 m (1,640 ft)
Dike Width	8 m (26 ft)
Extension of Dike Above Drift	300 m (980 ft)
Obstacles Total Length	290 m (950 ft)
Obstacles Total Height	1.8 m (5.9 ft)

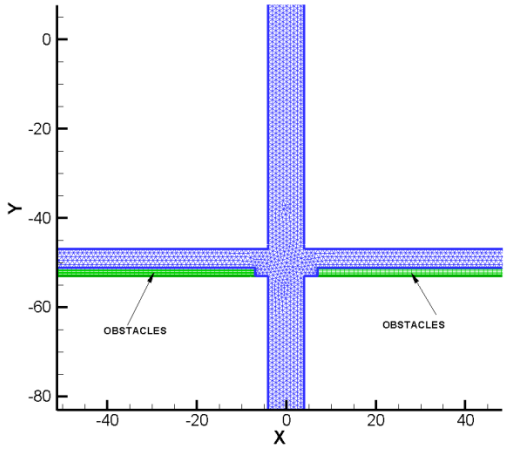

Fig. 2. Computational grid

TABLE II. Details of the Computational Grid

Construct	Grid Dimension ($N_x \times N_y$)*
Drift	20 × 500
Dike	600 × 15
Obstacles (each)	290 × 8
*N_x = Number of cells in the x-direction and N_y = Number of cells in the y-direction	

Tunnel walls were treated as isothermal, and wall-rock temperature was specified at a constant 300 K (80.33°F) (simulations reveal that no appreciable change occurred in the wall-rock temperature in the timespan considered). The obstacle temperature was specified as 350°K (170.33°F). The pressure inside the tunnel was treated as atmospheric, and in all the simulations, the tunnel was assumed to be initially filled with air. The subsurface tunnel is considered closed at both ends, but this assumption makes little difference to the flow behavior in the modeled grid.

IV. NUMERICAL METHOD

The commercial software FLUENT® Version 6.3[22] was used for the simulations. FLUENT uses a control-volume-based technique to convert a general scalar transport equation to an algebraic equation that is solved numerically. It has a pressure-based solver and a density-based solver. While the pressure-based solver is normally used for incompressible flows, the density-based solver is recommended for compressible high Mach number flows. For the present case (because it involves very low Mach number incompressible flow) the pressure-based solver is used. A variety of spatial and temporal discretization schemes, as well as turbulence models are also available in FLUENT. However, for the present simulations, based on the Reynolds number, the flow is in the laminar regime.

For these simulations, the solutions to the full two-dimensional Navier-Stokes equations were obtained using an unsteady, implicit approach. The volume of flow[23] approach was used to properly simulate the two-phase magma-air interface in the subsurface tunnel. The Semi Implicit Pressure Linked Equations–Consistent (SIMPLEC) algorithm was used to treat pressure-velocity coupling for stability. The third-order Monotone Upstream-Centered Schemes for Conservation Laws (MUSCL) were used to derive the face values of different variables for the spatial discretization, which was used to compute the convective fluxes. The upwind difference scheme was used for its enhanced numerical stability. The pressure-based solver was used in conjunction with a Green-Gauss cell-based gradient option. An implicit time marching scheme was used for faster convergence. Temporal discretization was achieved through a second-order implicit method (second-order backward Euler scheme). The Reynolds number (based on the magma viscosity and density) was 533, so the flow was considered laminar. The solutions were initiated in the unsteady mode. The air-magma interface was modeled using the volume of fluid method available in FLUENT. The timestep used for the unsteady simulations was varied between 0.01 and 0.05 seconds. The computations were conducted on a Sun Fire X4100 cluster configured with 10 dual-core AMD Opteron 200 series processors with 16 GB RAM per processor.

Properties of the interactive materials used in the simulations were obtained from Detournay, et al.[24] and are listed in Table III. The underground tunnel was assumed to be made of tuff. The magma properties are intended to simulate basaltic magma with a temperature of 1,450 K (2,150°F), the host-rock properties for a tuff is 300 K (80.33 °F), and the obstacle material at 350 K (160 °F). The magma temperature and viscosity are held constant in these simulations and latent heat of magma crystallization is not considered.

TABLE III. Materials and Properties Used in the Simulations

	Density		Specific Heat		Thermal Conductivity		Viscosity	
	Kg/m^3	lbm/ft^3	J/kg-K	BTU/lb-°F	W/m-K	Btu/(ft h °F)	Pa-s	$lbf\text{-}s/ft^2$
Magma	2,663	166.23	1,945	0.465	0.6	0.35	40	0.835
Air	1.225	0.0764	1,005	0.24	0.0242	0.014	1.78 e-05	3.72 e-07
Tuff	2,043	127.416	985	0.235	1.18	0.668	—	—
Obstacle Material	3,495	218	378	0.09	1.5	0.8491	—	—

In reality this would only impart a possible 1 percent increase in temperature in the time scale considered. The heating of air in the tunnel is not considered.

V. RESULTS AND DISCUSSIONS

To gain insights about the fluid flow field(s) occupying the dike and tunnel after intersection, simulations focused primarily on two scenarios: (i) magma initially entering and eventually filling a tunnel both with and without the presence of obstacles and (ii) a magma-filled tunnel including obstacles under conditions of constant magma supply and ascent (steady state) across the tunnel between the top and bottom dike intersections. In both scenarios, the velocity, vorticity, and calculation patterns that develop inside the horizontal tunnel were investigated.

Scenario (i) was investigated in configurations that included and excluded obstacles so that the effects of an obstacle on the floor of a tunnel could be ascertained. Under the presence of gravity and driven by pressure, single-phase (degassed) magma ascends the dike at 1 m/s (3.3 ft/s), intersects and intrudes into a tunnel, and begins filling the tunnel from the bottom [Figs. 3(a,b)]. As the tunnel is filling with magma, air is displaced and escapes up the dike and into the tunnel wall. Counterrotating vortices of air develop in the dike due to the temperature difference between the hot air and the cold air. Notice, too, a small volume fraction of air remains inside the tunnel after magma has completely filled the tunnel. This remnant air is the result of assuming a closed-end tunnel with zero permeability walls. However, these modeled residual air pockets and air behavior are not potentially significant to flow patterns because of the high difference of density between the magma and the air. Even though the air temperature potentially increases in contact with magma, because of this large density difference, the air does not influence the flow rate and turbulence (viscosity changes). In addition, in the current simulations, low speed effusive flow of magma was considered. As a result, shock and pressurized air slowing the flow down is not encountered in the current simulations. At the current low speed effusive magma flow, it is almost incompressible flow.

Magma continues its ascent up the dike once the tunnel is completely filled, and counterrotating vortices attributable to viscous coupling develop at the intersection of the dike and the tunnel in the magma. Beyond these small vortices in the magma adjacent to the dike, the larger circulation pattern established is characterized by magma flowing away from the dike along the lower portion of the tunnel and back toward the dike along the upper portion at very low velocities. In these simulations, magma ascending along the sides of the dike has a much lower velocity than magma ascending along the dike center, but this profile reflects the no-slip boundary condition applied to the dike walls. Figs. 3 (a) and (b) as well as figs. 4(a) and (b) demonstrate how these flow patterns develop without and with obstacles in the tunnel. However, in the current two-dimensional simulations, the obstacle is represented by a vertical slice. In some cases (as modeled here), the obstacle is circular in cross section, and magma could flowed through the sides and through the void on the top. But because of the 2-D simulations, those flow features are not predicted in the current work. In addition, the simulations conducted without obstacles predict the backflow of magma (toward the dike) in the lower portion of the tunnel. But the simulations with the obstacles are unable to predict the backflow of magma, because of the two-dimensional geometry considered in the simulations.

Given the previously described circulation inside a magma-filled tunnel, investigations performed for scenario (ii) (with obstacles) included variations in the distance between the dike and the obstacles and in the ascent rate of the magma. Figs. 5(a) and 5(b) illustrate changes in flow resulting from a distance of ~4 m (~13 ft) and ~7 m (~22.56 ft) between the dike and the end of the obstacles. At 4 m (13 ft), circulation in the tunnel and the velocity profile in the dike look much the same as Fig. 3(b). Both clockwise and counterrotating vortices develop in the magma-filled space between the dike and the obstacle, and a long, low-velocity cell develops in the tunnel beyond these vortices. However, if the space is increased from ~4 m (~13 ft) to ~7 m (~22.56 ft) [Fig. 5(b)], a second, more distinct clockwise vortex in the magma develops above the obstacles adjacent to the counterclockwise vortex that largely occupies the gap between the obstacle and the dike. As in the ~4 m

(~13 ft) case [Fig. 5(a)], these smaller vortices decrease away from the dike and are replaced by a larger low velocity cell. On the left hand side of the drift, we have a counterrotating vortex and in the right hand side we have a clockwise vortex. The colour bar in the figure represents the vorticity magnitude. Clockwise vortex is considered positive. The magnitude of the vortex is controlled by the viscous wall coupling and the rotation of the flowfield and magma enters the drift and encounters obstacles. In the simulation results shown in Fig. 6, magma velocity at the inlet was increased to 2 m/s and 3 m/s (6.6 and 9.8 ft/s) to examine its effect on the vorticity field. At 1 m/s (3.3 ft/s), the results are equivalent to those previously discussed [Figs. 4(b) and 5(a)]. With increasing magma ascent velocity, the strength and size of the primary, counterrotating vortices that occupy the space between the dike and the obstacle increase, and at 3 m/s (9.8 ft/s), two counterrotating vortices develop, one on top of the other, in the gap between obstacle and dike.

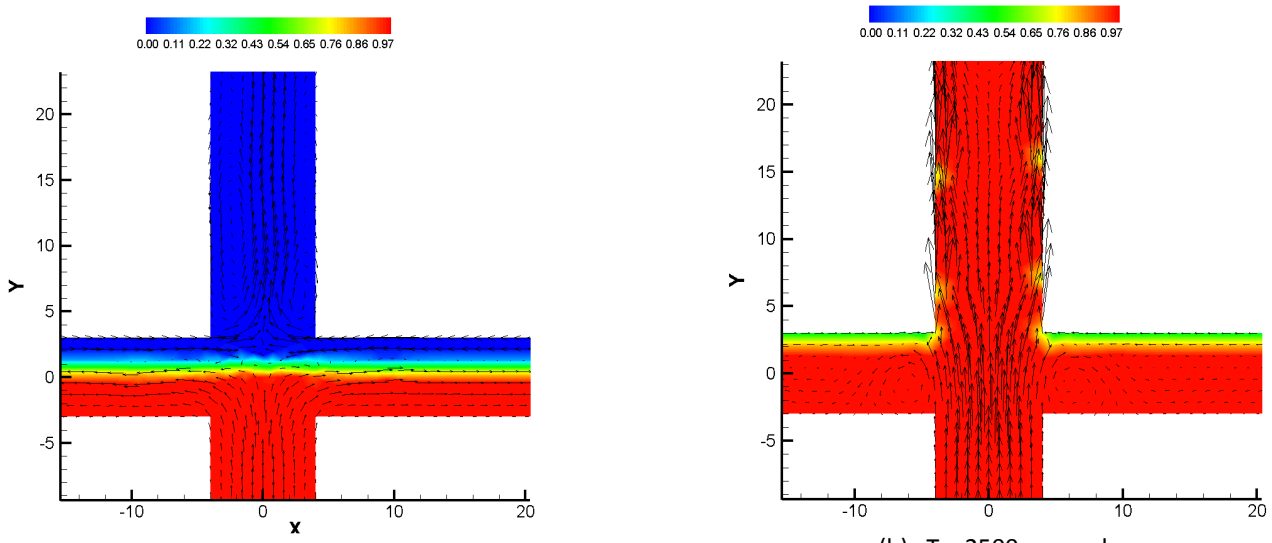

(a) T = 1000 seconds

(b) T = 2500 seconds

Fig. 3. Time sequence of magma filling drift without obstacles. Color contours show magma volume fraction superimposed with velocity vectors; magma inlet velocity = 1 m/sec (3.28 ft/sec); length is in meters.

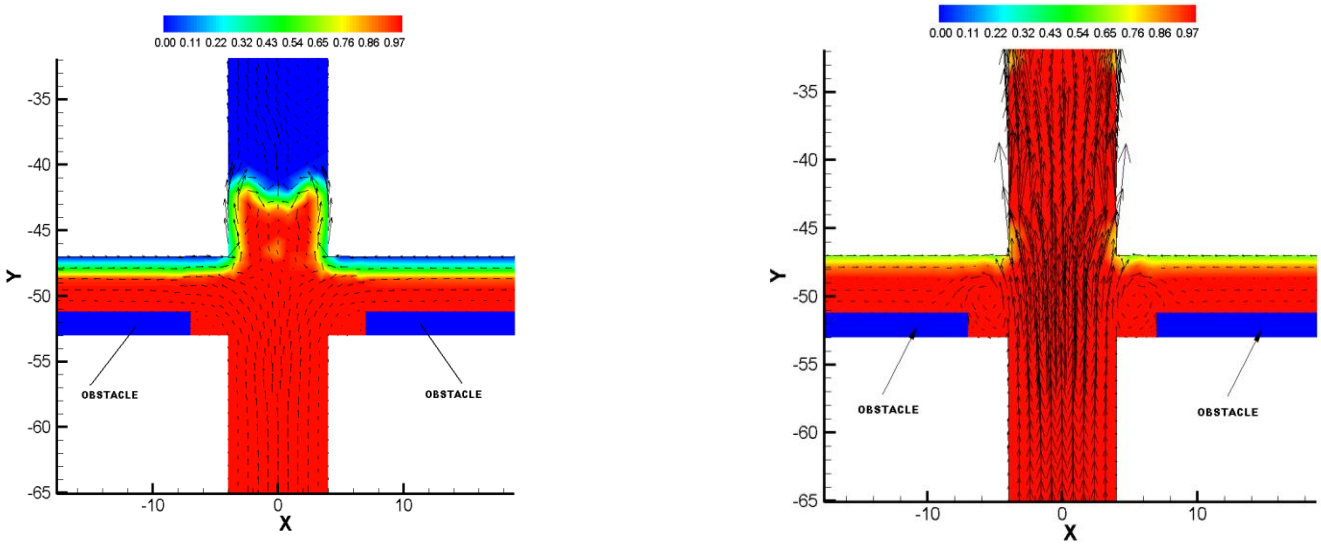

(b) T = 1000 seconds

(b) T = 2500 seconds

Fig. 4. Time sequence of magma filling drift with obstacle. Color contours show magma volume fraction superimposed with velocity vectors; magma inlet velocity = 1 m/sec (3.28 ft/sec); distance between dike and obstacle = 4 m (13.12 ft); length is in meters.

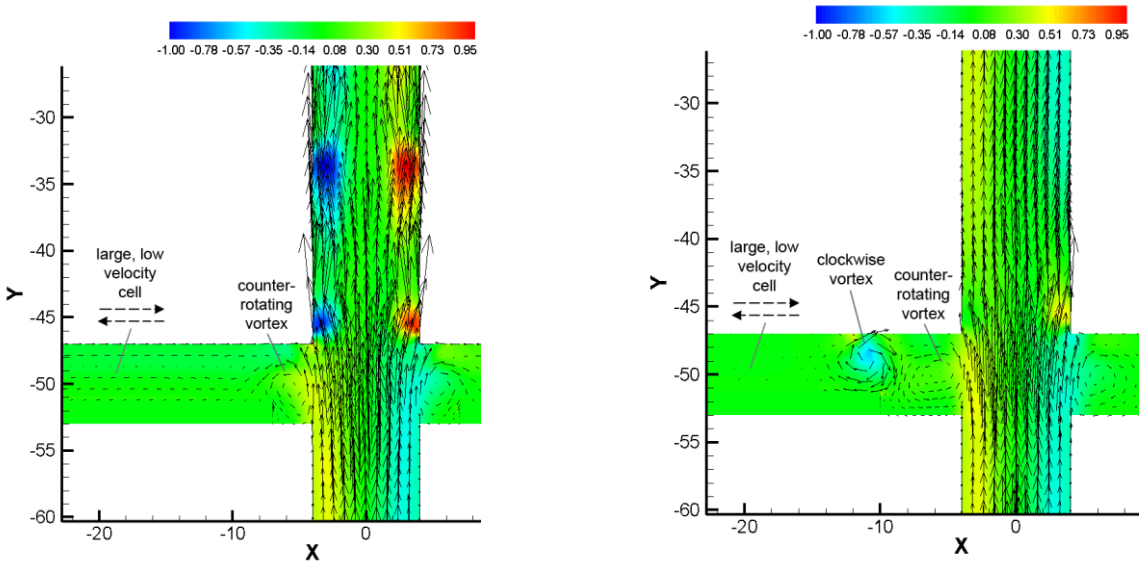

(a) Distance between dike and obstacle = 4 m

(b) Distance between dike and obstacle = 7 m

Fig. 5. Effect of distance between dike and obstacles on the flowfield. Color contours show vorticity superimposed with velocity vectors. Magma inlet velocity = 1 m/sec (3.28 ft/sec). length is in meters

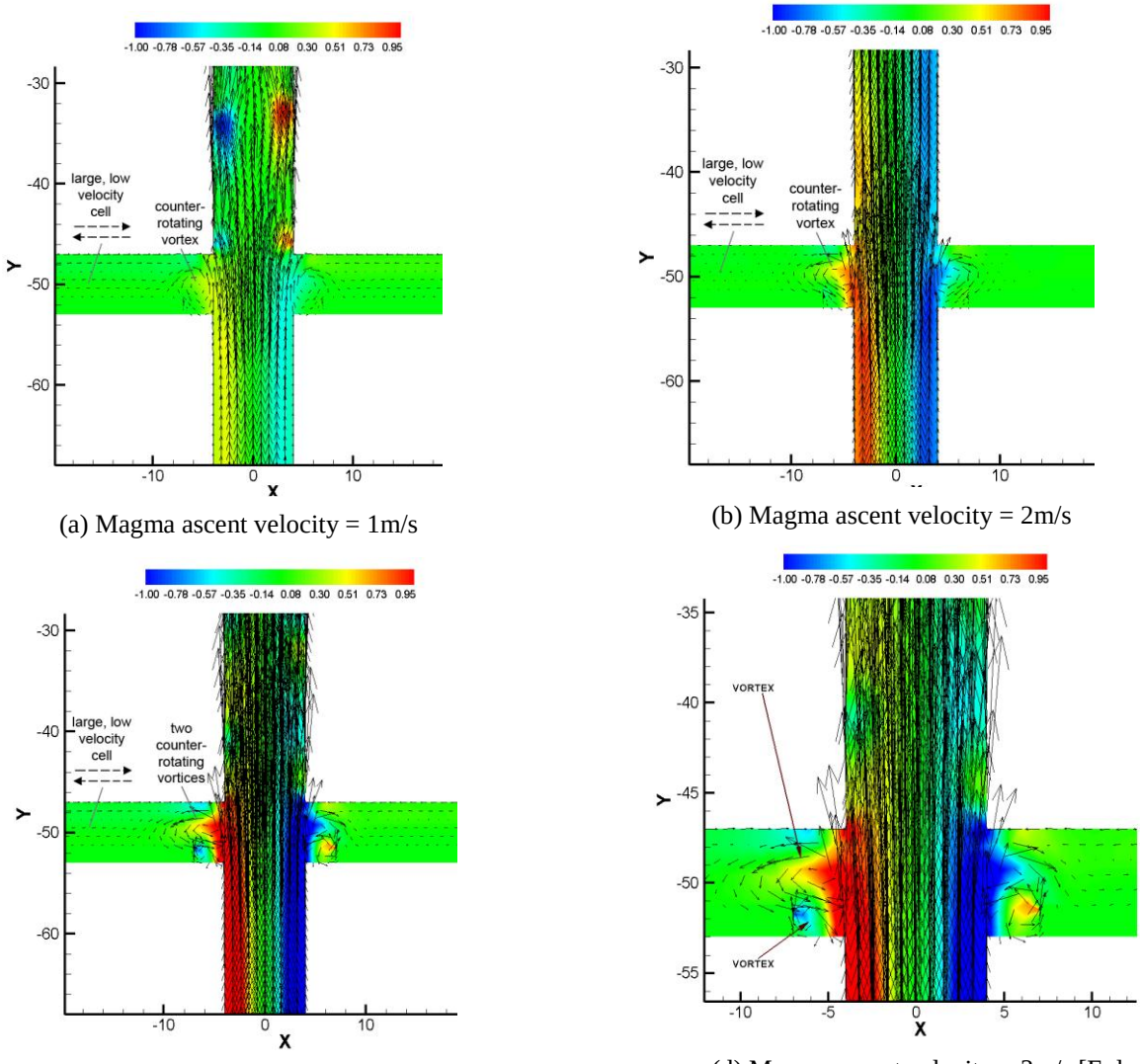

(a) Magma ascent velocity = 1m/s

(b) Magma ascent velocity = 2m/s

(c) Magma ascent velocity = 3m/s

(d) Magma ascent velocity = 3m/s [Enlarged]

Fig. 6. Effect of magma ascent velocity on flowfield: Color contours show vorticity superimposed with velocity vectors. Distance between dike and obstacle = 4 m (13.12 ft); length is in meters.

VI. CONCLUSIONS

We performed a numerical model study of the flow patterns that might develop in a dry subsurface tunnel intruded and transected by a dike of degassed (single-phase) basaltic magma, where the tunnel contains obstacles. This shows that the tunnel will fill with magma and provides a glimpse of the complex flow patterns that might develop in the tunnel near the dike under various conditions of magma supply rate and obstacle position. The/our results are broadly similar to those of an earlier experimental and theoretical study[15] with analog fluid, that also modeled slow intrusive degassed magma flow filling a horizontal space (without obstacles). Our two-dimensional simulation results show that magma flow patterns that develop within the tunnel are affected by the location of the dike intersection, relative to obstacles present in the tunnel. Under the conditions modeled in this study, low viscosity, nonexpanding magma ascending along a dike that intersects a tunnel will fill the tunnel under the influence of gravity from the base to the top and then continue upwards along the dike. Counterrotating vortices in magma adjacent to the dike that extend into the tunnel are driven by viscous coupling between the magma rising in the connected dike and the magma in the tunnel. In the tunnel beyond these primary vortices, a larger, low velocity circulation cell is established with magma flowing away from the dike along the base of the tunnel and toward the dike along the tunnel ceiling. This same pattern develops in the presence of an obstacle in the tunnel. Flow patterns that develop in a magma-filled tunnel can be affected by the location of dike intersection, specifically relative to obstacles in the tunnel. Slight changes in the modeled distance between the dike and the obstacles produced additional vortices adjacent to the primary vortices (i.e., those located directly next to dike position) that extended higher velocity circulating magma further down the tunnel. In addition to the strength and size of the primary vortices, the shape and distribution of the vortices that develop are affected by the ascent rate of the magma in the dike. At higher ascent rates, vertically coupled counterrotating vortices develop in the space between the dike and the obstacles. In all cases, some pattern of circulation developed in the tunnel, and the pattern was largely influenced by the interplay between the ascending magma and location of the obstacles.

ACKNOWLEDGMENTS

This paper is an independent product of the Center for Nuclear Waste Regulatory Analyses and does not necessarily reflect the view or regulatory position of the U.S. Nuclear Regulatory Commission (USNRC). The USNRC staff views expressed herein are preliminary and do not constitute a final judgment or determination of the matters addressed or of the acceptability of any licensing action that may be under consideration at the USNRC.

REFERENCES

1. R. J. RAMOS, "One-Dimensional, Time-Dependent, Homogeneous Two-Phase Flow in Volcanic Conduits," *International Journal for Numerical Methods in Fluids*, **21**, 253–278 (1995).
2. F. DOBRAN, "Nonequilibrium Flow in Volcanic Conduits and Application to the Eruptions of Mt. St. Helens on May 18, 1980, and Vesuvius in AD 79," *Journal of Volcanology and Geothermal Research*, **49**, 285–311 (1992).
3. F. DOBRAN and P. PAPALE, "Magma-Water Interaction in Closed Systems and Application to Lava Tunnels and Volcanic Conduits," *Journal of Geophysical Research*, **98**, 14041–14058 (1993).
4. D. N. KEATING, G. A. VALENTINE, D. J. KRIER, and F. V. PERRY, "Shallow Plumbing Systems for Small-Volume Basaltic Volcanoes," *Bulletin of Volcanology*, **70**, 563–582 (2008).
5. J. WILSON and J. W. HEAD, III, "Ascent and Eruption of Basaltic Magma on the Earth and Moon," *Journal of Geophysical Research*, **86**, 2971–3001 (1981).
6. P. PAPALE and F. DOBRAN, "Modeling of the Ascent of Magma During the Plinian Eruption of Vesuvius in AD79," *Journal of Volcanology and Geothermal Research*, **58**(1–4)**,** 101–132 (1993).
7. O. MELNIK, "Dynamics of Two-Phase Conduit Flow of High-Viscosity Gas-Saturated Magma: Large Variations of Sustained Explosive Eruption Intensity," *Bulletin of Volcanology*, **62**, 153–170 (2000).

8. P. PAPALE, “Dynamics of Magma Flow in Volcanic Conduits With Variable Fragmentation Efficiency and Nonequilibrium Pumice Degassing,” *Journal of Geophysical Research*, **106**, 11043–11065 (2001).
9. S. DARTEVELLE and G. A. VALENTINE, “Transient Multiphase Processes During the Explosive Eruption of Basalt Through a Geothermal Borehole (Namafjall, Iceland, 1977) and Implications for Natural Volcanic Flows,” *Earth and Planetary Science Letters*, **262**, 363–384 (2007).
10. A. NERI, A. DI MURO, and M. ROSI, “Mass Partition During Collapsing and Transitional Columns by Using Numerical Simulations,” *Journal of Volcanology and Geothermal Research*, **115**, 1–18 (2002).
11. J. DUFEK and G. W. BERGANTZ, “Transient Two-Dimensional Dynamics in the Upper Conduit of a Rhyolitic Eruption: a Comparison of Closure Models for the Granular Stress,” *Journal of Volcanology and Geothermal Research*, **143**, 113–132 (2005).
12. WOODS, A.W., S. SPARKS, O. BOKHOVE, A.M. LEJEUNE, C. CONNOR, and B.E. HILL. “Modeling Magma-Drift Interaction at the Proposed High-Level Radioactive Waste Repository at Yucca Mountain, Nevada, USA.” *Geophysical Research Letters*. **29**, 13, 19-1-19-4 (2002).
13. T. MENAND and J. C. PHILLIPS, “Gas Segregation in Dykes and Sills,” *Journal of Volcanology and Geothermal Research,* **159,** 393–408 (2007).
14. T. MENAND, J. C. PHILLIPS, R. S. J. SPARKS, and A.W. Woods, “Modeling the flow of basaltic magma into subsurface nuclear facilities”, in Volcanic and Tectonic Hazard Assessment for Nuclear Facilities, Edited by C. B. Connor, N. A. Chapman and L. J. Connor, Cambridge University Press, (2009).
15. T. MENAND, J. C. PHILLIPS, and R. S. J. SPARKS, “Circulation of Bubbly Magma and Gas Segregation Within Tunnels of the Potential Yucca Mountain Repository,” *Bulletin of Volcanology,* doi:10.1007/s00445–007–0179–5 (2008).
16. A. M. LEJEUNE, B. E. HILL, A. W. WOODS, R. S. J. SPARKS, and C. B. CONNOR, Intrusion dynamics for volatile-poor basaltic magma into subsurface nuclear installations”, in Volcanic and Tectonic Hazard Assessment for Nuclear Facilities, Edited by C. B. Connor, N. A. Chapman and L. J. Connor, Cambridge University Press, (2009).
17. A. M. LEJEUNE, A. W. WOODS, R. S. J. SPARKS, B. E. HILL, and C. B. CONNOR, “The Decompression of Volatile-Poor Basaltic Magma From a Dike into a Horizontal Subsurface Tunnel,” CNWRA, San Antonio, Texas (2002).
18. B. D. MARSH, and N. COLEMAN, “Magma Flow and Interaction With Waste Packages in a Geologic Repository at Yucca Mountain, Nevada,” *Journal of Volcanology and Geothermal Research*, **182**, 76–96 (2009).
19. Sandia National Laboratories, “Dike/Drift Interactions,” MDL–MGR–GS–000005, Rev. 02, Sandia National Laboratories, Las Vegas, Nevada (2007).
20. L. IBARRA, T. WILT, G. OFOEGBU, R. KAZBAN, F. FERRANTE, and A. CHOWDHURY, “Drip Shield-Waste Package Mechanical Interaction,” CNWRA, San Antonio, Texas (2006).
21. G. DANKO and D. BAHRAMI, “The Application of CFD to Ventilation Calculations at Yucca Mountain,” Proceedings of Waste Management 2002 Conference, Tucson, Arizona, February 24–28, WM Symposia, Inc., Tucson Arizona (2002).
22. Fluent, Inc., “FLUENT User Manual Version 6.2.16,” Fluent, Inc., Lebanon, New Hampshire (2006).
23. C. W. HIRT and B.D. NICHOLS, “Volume of Fluid (VOF) Method for the Dynamics of Free Boundaries,” *Journal of Computational Physics*, **39**, 201–225 (1981).
24. E. DETOURNAY, L. G. MASTIN, J. R. A. PEARSON, A. M. RUBIN, and F. J. SPERA, “Final Report of the Igneous Consequences Peer Review Panel, With Appendices,” MOL.20031014.0097, MOL.20030730.0163, Bechtel SAIC Company, LLC, Las Vegas, Nevada (2003).